PROCEEDINGS OF SCIENCE

The Crab Optical/X/gamma-ray polarisation processes

Jumpei Takata *Academia Sinica and National Tsing Hua University - Institute of Astronomy and Astrophysics - Taiwan
E-mail: takata@tiara.sinica.edu.tw

We investigate polarization of the radiation in optical to γ-ray energy bands from the Crab pulsar in the frame work of the outer gap accelerator. The recent version of the outer gap, which extends from inside the null charge surface to the light cylinder, is used for examining the pulse profiles, the position angle of polarization and the polarization degree. We compare the predicted polarization characteristic with the Crab optical data and the polarization in soft γ-ray bands measured by INTEGRAL. We show that the calculated polarization characteristics with the outer gap scenario are in general consistent with the Crab optical data after subtracting the DC level. With the observed high polarization degree, we suggest the off-pulse emissions measured by INTEGRAL are emitted outside the magnetosphere.

Polarimetry days in Rome: Crab status, theory and prospects
October 16-17, 2008
Rome, Italy

*Speaker.

PoS(CRAB2008)014

1. Introduction

Young pulsars are strong γ-ray sources. The EGRET had been measured the pulsed γ-ray emissions from 6 pulsars (Thompson 2004). The new γ-ray satellites, *Fermi* and *AGILE*, will increase number of the γ-ray pulsars in the next few years. The observed radiation properties, such as the pulsed profile and the spectra, will be useful for us to diagnose the particle acceleration ad the high-energy emission processes in the pulsar magnetospheres. The non-thermal processes have been discussed with the polar cap/slot gap model and the outer gap model in the literature (Harding et al 2008; Takata & Chang 2008).

Polarization measurement will play an important role to discriminate the various models, because it increases observed parameters, namely, polarization degree (p.d.) and position angle (p.a.) swing. So far, the optical polarization data for the Crab pulsar is available (Kanbach et al. 2005) in high energy bands. Because the electromagnetic spectrum of the pulsed emissions from the Crab pulsar is continuously extending from optical through γ-ray bands. We expect that the optical radiation process is related with the higher energy emission processes. *INTEGRAL* measured the polarization of the γ-ray emissions from the Crab pulsar for the first time (Dean et al. 2008). In the future, furthermore, the polarization of X-ray and soft γ-ray emissions from the Crab pulsar will probably be able to be measured by ongoing projects. These data will be useful for us to discriminate the different models. In this paper, we examine the optical polarization characteristics of the Crab pulsar with the outer gap accelerator model. We will discuss the polarization characteristics of the pulsed radiation in optical to γ-ray energy bands.

2. The Crab pulsar;outer gap scenario

The high-energy radiation taken place in outer magnetospheric acceleration region (outer gap) was proposed by Cheng et al. (1986). The outer gap accelerator model assumes a strong acceleration between the null charge surface of the Goldreich-Julian charge density and the light cylinder. The Goldreich-Julian charge density is described by $\rho_{GJ} \sim -\Omega B_z/2\pi c$ with Ω being the rotation frequency, B_z the magnetic field component projected to the rotation axis, and c the speed of light.

For the Crab pulsar, the charge particles are accelerated above 10 TeV by the electric field parallel to the magnetic field lines in the outer gap. The accelerated particles emit the "primary" γ-ray photons via the curvature radiation process. For the Crab pulsar, most of the primary photons will convert into so called "secondary" pairs outside the gap by colliding with synchrotron X-rays emitted by the secondary pairs. The secondary pairs emit optical - MeV photons via the synchrotron process and photons above MeV with the inverse Compton process. The high-energy photons emitted by the secondary pairs may convert into tertiary pairs at higher altitude by colliding with the soft X-rays from the stellar surface. The tertiary pairs emit the optical-UV photons via the synchrotron process. This secondary and tertiary photons appear as the observed radiations from the Crab pulsar

3. Polarization calculation

3.1 Acceleration and radiation process

We consider the outer gap geometry that is extending from inside null charge surface to near the light cylinder (Takata et al 2004). Because the Crab pulsar has a thin gap, we may approximately describe the accelerating electric field (Cheng et al. 1986) with

$$E_{||}(r) = \frac{\Omega B(r) f^2(r) R_{lc}^2}{cs(r)}, \tag{3.1}$$

where $f(r)$ is the local gap thickness in units of the light radius, $R_{lc} = c/\Omega$, and $s(r)$ is the curvature radius of the magnetic field line. The typical fractional size of the outer gap is given by $f(R_{lc}/2) \sim 5.5B^{-4/7}P^{26/21}$ (~ 0.04 for the Crab pulsar) and the local fractional size is estimated by $f(r) \sim f(R_{lc}/2)(2r/R_{lc})^{1.5}$ (Cheng et al. 2000).

The electric field described by equation (3.1) can be adopted for the acceleration beyond the null charge surface. Inside null charge surface, the electric field rapidly decreases because of the screening effects of the pairs. To simulate the accelerating electric field between the inner boundary located at r_i and the null charge surface, we assume the electric field with $E_{||}(r) = E_n(r/r_i)^2 - 1/(r_n/r_i)^2 - 1$, where E_n is the strength of the electric field at the null charge surface and r_n and r_i are the radial distances to the null charge surface and the inner boundary of the gap, respectively. Electrodynamically speaking, the position of the inner boundary r_i is determined with the electric current. On the other hand, the magnitude of the electric current in the gap depends on the global structure of the magnetosphere including the polar cap and wind zone. Therefore, in the present local model, we treat the r_i as the model free parameter. .

For the Crab case, the synchrotron radiation from the secondary pairs contribute to the The photon spectrum of the synchrotron radiation from the each radiation position is

$$F_{syn}(E_\gamma, r) = \frac{3^{1/2} e^3 B(r) \sin\theta_p(r)}{mc^2 h E_\gamma} \times \int \left[\frac{dn_e(r)}{dE_e}\right] F(x) dE_e dV_{rad}, \tag{3.2}$$

where $x = E_\gamma/E_{syn}$, E_{syn} is the typical photon energy, θ_p is the pitch angle of the particle, $F(x) = x\int_x^\infty K_{5/3}(y)dy$, where $K_{5/3}$ is the modified Bessel function of order 5/3, $dn_e/dE_e \propto E_e^{-2}$ is the distribution of the pairs and dV_{rad} is the volume element of the radiation region considered.

3.2 Stokes parameters

For a high Lorentz factor, we can anticipate that the emission direction of the particles coincides with the direction of the particle's velocity. In the observer frame, the particle motion may be described by

$$n = \beta_0 \cos\theta_p b + \beta_0 \sin\theta_p b_\perp + \beta_{co} e_\phi, \tag{3.3}$$

where the first term in the right hand side represents the particle motion along the field line, for which we use the rotating dipole field, and b is the unit vector of the magnetic field line. The second term in equation (3.3) represents gyration motion around the magnetic field line and $b_\perp \equiv \cos\delta\phi k + \sin\delta\phi k \times b$ is the unit vector perpendicular to the magnetic field line, where $\delta\phi$ refers

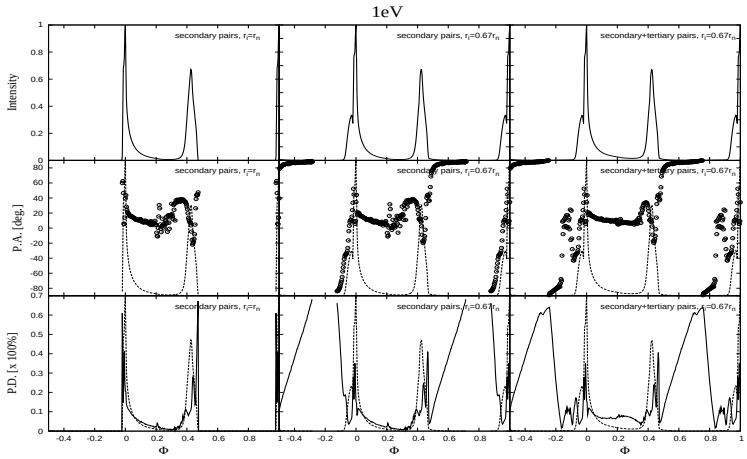

Figure 1: Polarization characteristics of optical radiations with the traditional model (left column) and the present model (right column). The upper, middle and lower panels in each column show, respectively, the light curve, the position angle and the polarization degree for $\alpha = 50^\circ$ (after Takata et al. 2007).

the phase of gyration motion and $k = (b\cdot\nabla)b/|(b\cdot\nabla)b|$ is the unit vector of the curvature of the magnetic field lines. The third term is co-rotation motion with the star, $\beta_{co} = \rho\Omega/c$. The emission direction of equation (3.3) is described in terms of the viewing angle measured from the rotational axis, $\xi = \cos^{-1} n_z$, and the rotation phase.

The radiation at each point linearly polarizes with degree of $\Pi_{syn} = (p+1)/(p+7/3)$, where p is the power law index of the particle distribution, and circular polarization is zero. The direction of the electric vector of the electro-magnetic wave toward the observer is parallel to the projected direction of the acceleration of the particle on the sky. In the present case, the acceleration with equation (3.3) is approximately written by $a \sim \beta_0\omega_B \sin\theta_p(-\sin\delta\phi k + \cos\delta\phi k\times b)$.

We define the position angle χ^i to be angle between the electric field E_{em} and the projected rotational axis on the sky. The Stokes parameters Q^i and U^i at each radiation is represented by $Q^i = \Pi_{syn} I^i \cos 2\chi^i$ and $U^i = \Pi_{syn} I^i \sin 2\chi^i$. After collecting the photons from the possible points for each rotation phase Φ and a viewing angle ξ, the expected p.d. and p.a. are, respectively, obtained from $P(\xi,\Phi) = \Pi_{syn}\sqrt{Q^2(\xi,\Phi)+U^2(\xi,\Phi)}/I(\xi,\Phi)$ and $\chi(\xi,\Phi) = 0.5\mathrm{atan}[U(\xi,\Phi)/Q(\xi,\Phi)]$.

We note that we also calculate the radiation and its polarization properties for the inverse-Compton process of the secondary pairs, which formula are explicitly described in Takata & Chang (2007). The inclination angle α and the viewing angles ξ measured from the rotational axis are the model parameters. As explained above, the radial distance r_i to the inner boundary is also a model parameter.

4. Results

Figure 1 summarizes the pulse profiles (top panels), polarization angles (middle panels) and the degree of polarization (lower panels) at 1 eV predicted by three different emission geometries. The left column summarizes the results for the traditional outer gap geometry. The middle and

right columns show the results for the radial distance of 67% of the distance to null charge surface $r_i = 0.67r$, and the right column is taking into account also the emissions from the tertiary pairs. The other model parameters are $\alpha = 50^\circ$, $a = 0.94$, and $\xi \sim 100^\circ$, where the viewing angle is chosen so that the predicted phase separation between the two peaks is consistent with the observed value $\delta\Phi \sim 0.4$ phase. In the present case, the two peaks in the light curve is associated with the one magnetic pole

Upon comparison the pulse profiles between the pulse profiles of the left and middle columns, we find that the radiations from the secondary pairs inside the null charge surface contribute to the off-pulse emissions. Therefore, we find that the emissions from the inside null charge surface contribute to the off-pulse emissions. The emissivity of the off-pulse emissions are $< 10\%$ of the peak flux. In side the null charge surface, the accelerating electric field is partially screened by the pairs. The resultant emissivity of the synchrotron radiation of the secondary pairs are small.

For the viewing angle $\xi \sim 100^\circ$, the radiations from all gyration phases contribute to the observed radiation at the bridge phase, because the line of sight passes through middle part of the emission regions. In such a case, the depolarization is strong, and as a result, the emerging radiation from the secondary pairs polarizes with a very low p.d. ($< 20\%$) as lower panels in Figure 1 shows. Near the peaks, on the other hand, the radiations from the some range of gyration phases are not observed because the line of sight passes through the edge of the emission regions at peaks. Therefore, the depolarization is weaker and the emerging radiation highly polarizes.

We find from the middle panels in Figure 1 that the large swings in the polarization angle appear at the both peaks. The results (middle and right columns) of the new outer gap geometry predicts that the difference of the position angle between the off-pulse and the bridge phases is about 90 degree. We can see the effects of the tertiary pairs on the polarization characteristics at the bridge phase. By comparing the p.d. between middle and right panels, we find that tertiary pairs produce the radiations with $\sim 10\%$ of the polarization degree at the bridge phase.

The polarization characteristics (right column in Figure 1) predicted by the recent outer gap model are in general consistent with the Crab optical data after subtraction of the DC level (Kanbach et al. 2005). In particular, the model reproduces the most striking feature in the observed p.a. that the large swing at both peaks, and the observed low p.d. at bridge phase $\sim 10\%$. Also, the pattern of the degree of the polarization are reproduced by the present model.

Figure 2 shows the predicted polarization characteristics for higher energy bands. The model parameters are same with those for the right column in Figure 1. We can see that the calculated polarization characteristics in hard X-ray (left column in Figure 2) and soft γ-ray (right column in Figure 2) are similar with those in the optical bands. This is because the synchrotron radiation from the secondary pairs produces the radiation in optical through soft γ-ray energy bands.

As Figure 2 shows, the predicted angle of polarization in off-pulse emission in γ-ray bands is about ± 90 degree, which means the polarization angle is perpendicular to the direction of the rotational axis on the sky (0 degree). The result does not produce about 0 degree of the polarization angle measured by INTEGRAL (Dean et al. 2008). On the other hand, the polarization properties measured by INTEGRAL are similar to those of the optical DC emissions. This implies that the emission region of the optical DC level is also origin of the off-pulse γ-ray emissions. Because our model implies that the optical DC level emissions does not originate from the outer gap, we suggest that the off-pulse emissions observed by INTEGRAL would come from another region (e.g. wind

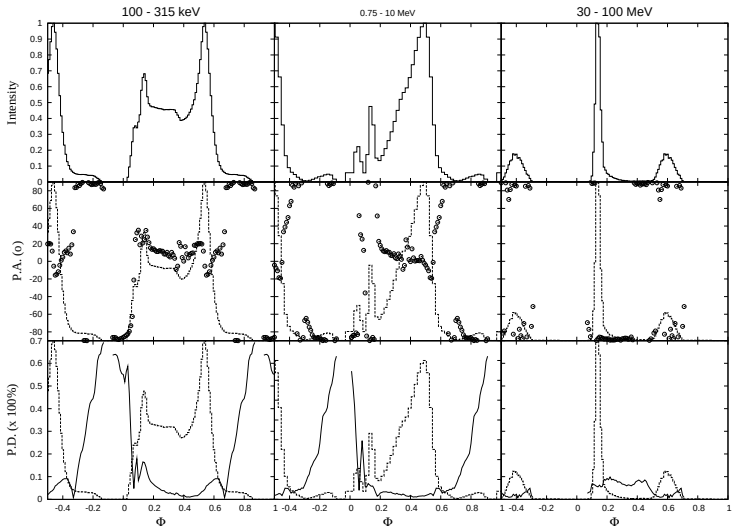

Figure 2: Polarization characteristics of radiations in hard X-ray and soft γ-ray bands.

zone or synchrotron nebula).

In summary, we calculated the polarization process in optical to γ-ray bands with the outer gap scenario for the Crab pulsar. We found that the outer gap model can explain the observed polarization characteristics of the optical data after subtracting the DC level. On the other hands, the present model does not explain the INTEGRAL data of the off-pulse emissions. We suggest that the off-pulse emissions measured by INTEGRAL come from outside magnetosphere.

References

[1] Cheng K.S., Ho C. & Ruderman M. 1986, ApJ, 300, 500

[2] Cheng K.S., Ruderman M. & Zhang L. 2000, ApJ, 537, 964

[3] Dean et al., 2008, Sci, 321, 1183

[4] Harding A.K., Strickman M.S., Gwinn C, Dodson R., Moffet D. & McCulloch P., 2002, ApJ, 576, 376

[5] Kanbach G., Słowikoska A., Kellner S. & Steinle H., 2005, AIP Conf. Proc. Vol.801, p.306

[6] Takata J., Shibata S. & Hirotani K. 2004, MNRAS, 354, 112

[7] Takata J., Chang H.-K. & Cheng K.S., 2007a ApJ, 656, 1044

[8] Takata J. & Chang H.-K., 2007b ApJ, 670, 677

[9] Takata J., Chang H.-K. & Shibata S., 2008, MNRAS, 386, 748

[10] Thompson D.J., 2004, in Cheng K.S., Romero G.E., eds, Cosmic Gamma Ray Sources. Dordrecht, Kluwer, p. 149